spe INJECTION MOLDING
Injection Molding Division
Molding Views

Spring 2024 | No. 122 www.injectionmoldingdivision.org Keep the connection! Join us on:

Chair's Message Jeremy Dworshak

Dear Members of the Injection Molding Division (IMD),

What a difference six months can make! It feels like just yesterday when we gathered to plot our strategic plan for the IMD. Today, I'm thrilled to report that significant progress towards our joint goals is underway.

Our strategic initiatives, spearheaded by dedicated leaders, are shaping up to be pillars of strength for our division. Workshops, led by David Kusuma & Chad Ulven, sustainability efforts, under the guidance of Davide Masato & Monika Kleczek, and communication initiatives, driven by Angela Rodenburgh & Erik Foltz, are gaining momentum and will be showcased at this year's Week of Injection Molding.

Keep an eye out for upcoming details on the Week of Injection Molding on our social media channels. The communication team is creating new ways of keeping all of us more engaged and informed on the happenings of the IMD.

ANTEC in St. Louis was an incredibly rewarding experience for me personally. I had the opportunity to delve into the intricacies of 2-stage screws and their application in injection molding—including in-person discussion with the researcher that conducted the work! Isn't that one of the great strengths of ANTEC and SPE? The learning opportunities are that much better when in-person networking is part of it. I feel truly grateful to have been at ANTEC and picked up this little 'golden nugget' of information.

The next few months will be filled with planning and executing our strategic plan, yet I have every confidence that our leadership team is prepared for the challenge ahead! I am also preparing to pass the leadership baton to David Kusuma, IMD's next chair, at the end of June. Just in time for my birthday!

Lastly, I invite you all to consider stepping up and joining the IMD board. We are always on the lookout for passionate individuals who are willing to contribute their time and expertise to furthering our mission.

Thank you for your continued support and dedication to the IMD!

Sending my best,

Jeremy Dworshak Chair,
Jeremy K. Dworshak Chair, Injection Molding Division (IMD) Society of Plastics Engineers (SPE)

IN THIS ISSUE:

MAY 2024

SPE WEBINAR: INTRODUCTION TO PROCESS AND THERMAL STABILIZATION IN POLYOLEFINS AND ENGINEERING POLYMERS

WEDNESDAY, MAY 1, 2024 11:00 AM (EDT) - 12:00 PM (EDT)
VIRTUAL EVENT
For more information: https://www.4spe.org/i4a/pages/index.cfm?pageID=8559

SPE ONLINE COURSE: INTRODUCTION TO TECHNICAL ENTREPRENEURSHIP: ESSENTIAL TOOLS FOR NPE AND OTHER INDUSTRY EVENTS

FRIDAY, MAY 3, 2024 11:00 AM (EST) - 12:00 (EST)
VIRTUAL EVENT
For more information: https://www.4spe.org/i4a/pages/index.cfm?pageID=8837

NPE2024 THE PLASTICS SHOW

MONDAY, MAY 6, 2024 9:00 AM (EST) - FRIDAY, MAY 10, 2024 3:00 PM (EST)
ORANGE COUNTY CONVENTION CENTER, ORLANDO, FLORIDA
For more information:
https://npe2024.mapyourshow.com/8_0/floorplan/?st=keyword&sv=SPE&hallID=W&selectedBooth=WL15

SPE WEBINAR: THE COMING PFAS LITIGATION RISK FOR PRODUCT MANUFACTURERS

FRIDAY, MAY 10, 2024 11:00 AM (EDT) - 12:00 PM (EDT)
VIRTUAL EVENT
For more information: https://www.4spe.org/i4a/pages/index.cfm?pageID=8562

AUTO EPCON CONFERENCE 2024

TUESDAY, MAY 14, 2024 8:00 AM (EDT) - 5:00 PM (EDT)
DETROIT MARRIOTT - TROY, 200 W BIG BEAVER, TROY, MI 48084
The SPE Detroit, SPE Injection Molding and SPE Additive Manufacturing chapters are hosting the Auto EPCON Conference 2024 on May 14, 2024 at the Detroit Marriott - Troy Hotel, 200 Big Beaver Rd, Troy, MI 48084.
For more information: https://www.4spe.org/i4a/pages/index.cfm?pageID=8601

JUNE 2024

INJECTION MOLD DESIGN - UMASS LOWELL PLASTICS ENGINEERING SEMINAR

MONDAY, JUNE 3, 2024 8:30 AM (EST) - WEDNESDAY, JUNE 5, 2024 5:00 PM (EST)

UMASS LOWELL, 185 RIVERSIDE ST., LOWELL, MA

This three-day seminar on Injection Mold Design should give those involved in the thermoplastics injection molding industry a strong fundamental understanding of tooling technology and the underlying engineering principles in the areas of melt flow, cooling, part ejection and mold structure.

For more information: https://gps.uml.edu/professional-training/plastics/seminars/injection-mold-design.cfm

SPE WEBINAR: INTRODUCTION TO STABILIZATION OF PVC FORMULATIONS

MONDAY, JUNE 10, 2024 11:00 AM (EDT) - 12:00 PM (EDT)

VIRTUAL EVENT

For more information: https://www.4spe.org/i4a/pages/index.cfm?pageID=8564

POLYMERIC MATERIALS: COMMODITY PLASTICS, ENGINEERING RESINS AND SPECIALTY POLYMERS - UMASS LOWELL PLASTICS SEMINARS

MONDAY, JUNE 17, 2024 8:30 AM (EST) - THURSDAY, JUNE 20, 2024 5:00 PM (EST)

UMASS LOWELL, 185 RIVERSIDE ST., LOWELL, MA

This program provides an overview of the many different families of commercially available polymeric materials. It also examines the basic concepts of polymerization through structure/property relationships and post-reactor modification, value-added compounding, important thermomechanical properties, design considerations, fundamentals of the various processing schemes, and material selection criteria for commercial end-uses.

For more information: https://gps.uml.edu/professional-training/plastics/seminars/polymer-materials-commodity-engineering-resins.cfm

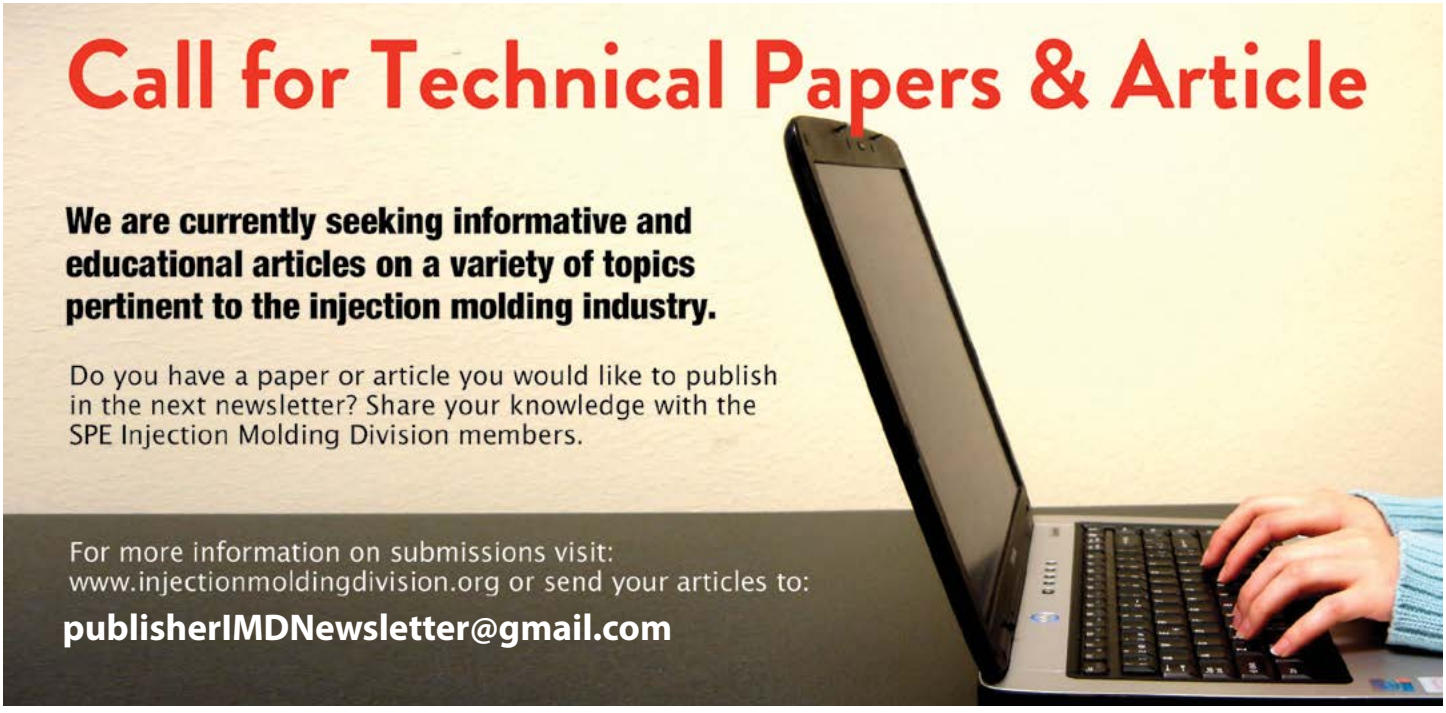

ANTEC® ReCAP

The event was the second in-person ANTEC® since the pandemic forced virtual presentations of the annual gathering in 2020 and 2021. While this year's turnout was a bit less than one-half of the pre-pandemic registration posted at ANTEC 2019 in Detroit, attendee numbers were received with enthusiasm by SPE. "We're very happy," said COO Sue Wojnicki.

The conference also attracted a larger number of papers for presentation than last year—285, according to Dr. Iván D. López, SPE's new director of technical programs, who oversaw the conference sessions. Last year, López noted, just over 150 papers were received.

The sources of the papers were also more diverse. ANTEC® usually attracts most of its research-intensive papers from academia, government laboratories and other specialized sources. Organizers are working to broaden submissions from industry. This year, López said, academic papers accounted for 60 percent of the total, while those sourced from industry represented 40 percent.

SPE and López want conference content to include more R&D and applications technologies from business. The plastics industry, he has said, faces challenges in many areas, especially the use and disposal of its products. Broadening conference content to include developments that are or will soon be commercial will boost the relevance and value of ANTEC® and the information it provides to attendees.

Celebrating SPE's 2024 Fellow of the Society Award Recipients

In early January, SPE announced the 2024 recipients of its Fellow of Society Award. The Fellow of the Society program was established in 1984 and 365 SPE members have been awarded with the Fellow title since its inception.

The Fellow of Society program honors SPE members for their outstanding contributions in the field of plastics engineering, science/technology, or in the management of such activities. Candidates must be sponsored by an SPE Section, Technical Division or Interest Group and elected by the Fellows Election Committee based on their professional record as well as written sponsorships from at least two SPE members.

The following plastics professionals received SPE's Fellow of Society Award for 2024:

DR. PETER FRENKEL
Vice President-Technology
Galata Chemicals

DR. WENYI HUANG
Principal Research Scientist
DuPont

DR. HARRY MAVRIDIS
Director of Product Development & Circular Design
Americas
Lyondellbasell

DR. JEFF MUNRO
Senior Research Scientist
DOW Chemical Company

DR. SRIKANTH PILLA
Professor and Director,
Center for Composite Materials
University of Delaware

DR. LI-YING TAMMY YANG
Research Fellow
GAF

Celebrating SPE's 2024 Honored Service Member Award Recipients

In January, SPE announced the 2024 recipients for its prestigious Honored Service Members Award. The SPE Honored Service Member program started in 1992 with 357 members named Honored Service Members since the program was launched.

To be elected an Honored Service Member, a candidate shall have demonstrated long-term, outstanding service to, and support of, SPE and its objectives, and shall be sponsored, in writing, by the Board of Directors of at least one Section, Division or Interest Group.

The following professionals received the SPE Honored Service Member Award for 2024:

JEFFREY S. DRUSDA
Technical Service Principal Scientist
The Chemours Company

PIERRE R. MOULINIÉ
Global Technical Marketing Head, Healthcare for
Engineering Plastics
Covestro

DAVID A. OKONSKI
Engineering Manager
IACMI-The Composites Institute

SAVE THE DATE!

National Week of Injection Molding

Tuesday, September 24, 2024 &
Wednesday, September 25, 2024

All Day Online

Navigating the Nano Challenge: Breakthrough Dispersion Technology

NEMO is changing the plastics industry with its innovative NemoBLEND masterbatches. This solution utilizes carbon nanotubes to enhance electrical conductivity, electromagnetic shielding, and lightweight, sustainable design

Noa Albocher. Founder & Editor +972-52-399-0860
PlasticTime

In the ever-evolving landscape of materials science, nanomaterials, particularly carbon nanotubes, have long been heralded as the "next generation" of advanced materials. Their vast potential lies in the capacity to impart exceptional properties to the matrices in which they are incorporated, particularly in terms of superior electrical conductivity. However, a significant challenge arises in realizing these properties, as nanoparticles tend to exhibit a natural inclination to form agglomerates.

Within this quest for groundbreaking solutions, enters NEMO Nanomaterials, a pioneering startup. Specializing in a distinctive compounding method for nanoparticles, the company has perfected a proprietary processing technique of SWNCT (Single-Walled Carbon Nanotube) hybrid.

The NemoBLEND can seamlessly integrate into any polymeric matrix, granting plastics with remarkable electrical conductivity properties and electromagnetic shielding capabilities suitable for a diverse range of applications.

NemoBLEND – Conductive masterbatch based on SWCNT.

Enhanced Conductivity and Versatility

The innovative masterbatches are currently available in four polymer-carriers: polyethylene, polypropylene, polystyrene, and various polyamides (nylon). Despite the high concentration of carbon tubes loaded into the masterbatch, the final product requires a low dosage—ranging from 10% to 30%, a notable advantage over alternative solutions.

Electric conductivity and EMI shielding for various applications with NemoBLEND.

Conductive and colorful: sample chips and molded parts with NemoBLEND combined with color pigments.

With volumetric electrical conductivity ranging from 10^2 to 10^9 [Ω·cm] and surface conductivity between 10^2 and 10^9 (Ω/sq), these masterbatches find diverse applications in cables, flexible piping, metal part replacements, crates, sockets and more. Their versatility extends across various industries such as automotive, medical, aviation, electronics, infrastructure, construction, energy, and communication. Moreover, NemoBLEND masterbatches can be processed in different methods, including injection, extrusion, and thermoforming. A notable advantage lies in the ability to combine the conductive additive with pigments, offering design freedom and the creation of colored products—a unique feature that competitors who are solely available in black cannot provide. NemoBLEND not only sets new standards for conductivity but also opens up possibilities for innovative and aesthetically diverse plastic applications.

From Lab to Life

The impact of NemoBLEND extends beyond the confines of the laboratory, finding practical applications across various industries with remarkable benefits. For instance, the incorporation of NEMO masterbatches in a plastic radar cover designed for electromagnetic shielding at frequencies ranging from 75 to 110 GHz resulted in weight savings of 40% compared to a traditional metal cover.

In the automotive sector, NemoBLEND plays a crucial role in the development of a flexible pipe for transporting flammable liquids. This innovative solution not only boasts excellent mechanical properties but also possesses the unique ability to discharge electrostatic charges, thereby ensuring enhanced safety and an extended lifespan.

Within the cable industry, NemoBLEND's influence is evident in the manufacturing of a plastic tube for cable braids that facilitates information transmission. This design not only provides electromagnetic interference (EMI) shielding but also eliminates the necessity for a previously essential metal layer. The outcome is a simplified tube featuring a reduced cross-sectional area and enhanced flexibility, ultimately streamlining the production process. Additionally, the incorporation of flame-retardant additives adds another layer of versatility to the product, further expanding its potential applications.

Partnering with Kafrit Group

In the industrial production process, NEMO receives invaluable assistance from Kafrit Group, known in the plastics industry for its compounding capabilities, additives and masterbatches. Notably, Kafrit has also made a significant investment in NEMO.

"Kafrit's strategic collaboration with NEMO extends far beyond mere financial investment. We provide essential support in marketing and sales, offering financial and regulatory advice within the international plastics landscape, and serving as a crucial manufacturing arm. Our partnership is not just about funding; it's about a deep connection and shared vision for innovation and growth in the dynamic plastics industry," affirms Daniel Singer, CEO of Kafrit Group.

Smart Foams Generated Via Supercritical Carbon Dioxide

John Daguerre-Bradford and Alan J. Lesser, University of Massachusetts Amherst, Conte Polymer Research Center, MA

Natural and synthetic polymeric foams display a variety of open and closed pores with diverse shapes, sizes, and degrees of anisotropy. In state-of-the-art foaming processes, microcellular anisotropy is generated by releasing confinement in one or more directions during the expansion of an initially isotropic melt or resin. As a result, the entire monolith foamed in this way exhibits cells aligned in the direction dictated by the confinement. This, in turn, results in a uniform deformational response that is dictated by the loading condition relative to the microcellular orientation.

In this work, investigation was performed into generating a foamed morphology within an anisotropic medium (e.g. film or fiber) to understand how molecular orientation affects the resulting anisotropy in the microcellular structure. Additionally further investigation into the use of this strategy to generate complex microcellular hierarchical constructs was performed by using fibers and or films as templates to understand their effect on the corresponding deformation. Herein, results are presented to show how assemblies of fibers are woven or twisted with a bias or helical structure and then foamed using superheated water (shH2O) and/or supercritical carbon dioxide ($scCO_2$) to manufacture complex microcellular structures. In addition, results from mechanical tests also show how the imposed bias in the foams result in complex deformation imposed by the bias. That is, foams generated to create a helical bias are shown to undergo torsional deformation commensurate with uniaxial deformation when compressed uniaxially. These concepts propose a technology to manufacture "smart foams" by assembling templates (films and/or fibers) that have locally different molecular orientations that ultimately create locally changing anisotropic microcellular patterns that govern complex deformational behavior under applied loads.

Introduction

Polymeric foams are a class of cellular materials that display a wide array of open or closed pores, with diverse shapes and sizes that are often anisotropic in practice [1]. Anisotropy in cellular solids stems from structural anisotropy of the cells or material anisotropy of the cell walls [2]. Structural anisotropy originates from the cells having,elongation along an axis while material anisotropy originates from thinner walls between cells following along an axis [2]. Regardless of the form of anisotropy, anisotropic foams, demonstrate a simple deformational response that is dictated by the loading condition relative to the microcellular orientation. Due to this, anisotropy within foams has been exploited to better suit a wide array of applications [3].

Some of the state-of-the-art foaming processes include chemical vapor deposition, freeze casting, and addition of chemical blowing agents [4-7]. In these processes, structural or material anisotropy is produced from an isotropic melt or resin, and an imposed confinement in one or more directions, generating anisotropic expansion [1-8]. Consequently, the cellular alignment for the entire foam is unidirectional which is dictated by the confinement. Unidirectional anisotropy within polymeric foams results in simple deformational respons-

es. Anisotropic foam properties vary due to the loading conditions relative to the microcellular orientation, however the mechanism of deformation remains the same.

One method for generating polymer foams is through gas-foaming, predominantly with supercritical CO_2 ($scCO_2$). This process has been used to generate foams from semicrystalline thermoplastic polymers such as poly(ethylene terephthalate) and polypropylene, from the melt state [9, 10]. A similar foaming method, solid-state gas-foaming, occurs when the polymer is saturated with a physical blowing agent like $scCO_2$ at high pressures and ambient temperatures. After saturation the sample is heated above the glass transition initiating cell growth, which stops when the sample is quenched [11-17]. This foaming method has been studied on a variety of amorphous thermoplastic polymers such as polystyrene, polyethersulfone, polyetherimide and polysulfone to name a few [11-13]. This method has also been studied on traditionally semi-cyrstalline polymers that were foamed in the amorphous sta te such as poly(ethylene-2,6-naphthalate) and poly(ethylene terephthalate) and semicrystalline thermoplastics in the semicrystalline state such a s poly(ε-caprolactone) and poly(lactic acid) [13-17]. This foaming method, however, does not produce anisotropic cells because the samples are not confined during cell nucleation and growth. Also, to our knowledge, investigation into how the molecular orientation of the semicrystalline polymers affects foaming, has not been studied.

Solid-state gas-foaming can be altered to simplify the process and allow for more control over the microcellular structure for semicrystalline polymers. Saturating polymers with $scCO_2$ above the glass transition but below melt at higher pressures in a confined system provides easy tuneability of the concurrent structure. Changes in pressure, temperature, time, and the addition of solvents, such as superheated water (shH_2O), can affect the density, cell size, cell shape and open or closed cell structure [18, 19]. This technique can be employed on oriented semicrystalline polymers to evaluate if the molecular orientation has an effect on the microcellular anisotropy.

This paper examines the creation and characterization of polymeric "sma rt foams" generated via solid-state gasfoaming using $scCO_2$ and shH_2O. This is done by foaming molecularly oriented anisotropic media (e.g. film or fiber) and studying the resulting effect on the anisotropy in the microcellular structure. This strategy is then utilized to produce complex microcellular hierarchical constructs by implementing a helical bias or weave onto assemblies of fibers, and studying the resulting microcellular structures and corresponding deformation. The subsequent polymeric foams exhibit complex deformation imposed by the bias i.e., a fiber assembly foamed with a helical bias undergoes torsional deformation commensurate with uniaxial deformation when compressed unia xia lly, resulting in a "sma rt foam".

Materials & Methods

Trilene Big Game 30lb, 0.56 mm diameter monofilament fishing line was purchased from Berkley Fishing and found to be polyamide 6 (PA6). The fiber and samples were stored in atmospheric moisture conditions before testing. PA6 chemical structure is outlined in **Figure 1**. CO_2 was obtained from Airgas. The water used was purified through reverse osmosis.

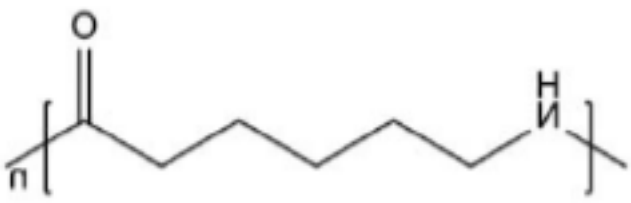

Figure 1: Polyamide 6 chemical structure.

Trilene Big Game Monofilament Analysis:

Differential scanning calorimetry (DSC) was performed on a TA Instruments Q200 DSC in aluminum pans. Heat/cool/heat experiments from 0 to 250 °C at 10°C/min to determine crystallinity of Trilene big game monofilament.

Fourier Transform Infrared (FTIR) spectra were recorded with a Perkin-Elmer Spectrum One Fourier transform infrared spectrometer directly on unmodified monofilament and PA6 pellets.

Wide Angle X-Ray Scattering (WAXS) was conducted using a SAXSLAB Ganesha 300XL next genera tion SAXS system with CuKα ra dia tion. Each measurement was performed at a q-range of 0.6 – 2.9 Å for 180 s. Spectra were collected for the Trilene monofilament. The 2D WAXS pattern raw data was used to calculate the Herman's orienta tion fa ctor, f, to get va lues for crystal orientation with the following equation [20]:

$$f = \frac{3*\langle cos^2\delta\rangle - 1}{2} \quad (1)$$

Where $\langle cos^2\delta\rangle$ is the mean cosine square of the diffracted plane intensity in reference to sample coordinate axis system and can be calculated as:

$$\langle cos^2\delta\rangle = \frac{\int_0^{\frac{\pi}{2}} I_\Delta * cos^2\delta * sin\delta \; d\delta}{\int_0^{\frac{\pi}{2}} I_\Delta * sin\delta \; d\delta} \quad (2)$$

Where I_Δ is the average signal intensity and δ is the degree of orientation of that intensity value in radians.

Foaming Procedure:

Foaming was performed in cylindrical high-pressure reactors, that can heat and pressurize with CO_2 simultaneously. The Trilene Big Game monofilament, which was found to be PA6, was wound 30 times forming a bundle of 60 fibers. The fiber ends were tied off and then placed into a helical twist bias with constant known tension of 1 kg. To maintain this helical twist bias during foaming, a fixture was developed that maintained the rotations and tension. The fiber bundle was 7 cm long and 0.6 cm in diameter, with the ability to change the number of initial rotations from 0 to 3 full rotations. The fixture was then filled with water and placed inside of the reactor and water was added up to 1 cm below the top of the reactor and closed. Fiber bundles were then foamed with conditions shown in **Table I**. After foaming the fibers sintered together creating one monolithic cylindrical sample with the same diameter as the test tube of 1 cm.

Table 1: Foaming conditions for PA 6 fiber bundles

Initial Rotations	Avg Pitch (radians)	Pressure (MPa)	Temp. (°C)	Time (Hr)
2	0.30	20.7	108	4
0	0	41.4	128	4
1	0.15	41.4	125	4
2	0.30	41.4	123	4
3	0.45	41.4	123	4

Polyamides undergo a melt temperature depression when processed in shH_2O therefore low processing temperatures can be used [21]. Foaming temperatures and pressures were varied to increase the processing window based on scCO_2 solubility. Samples foamed at higher pressures and temperatures were more reproduceable based on the increase in scCO2 solubility parameter [22,23].

The average pitch for the fibers in each bundle were calculated assuming that the fibers in the very center of the sample were not rotated but only twisted and the outer most fibers were rotated the full number of rotations as shown in **Figure 2**. The average pitch, p in radians (rad.) was calculated using Equation 3

$$p = \frac{\left(\frac{\int_0^r f_{*\pi r^2 dr}}{\pi r^2}\right) * R_0}{L_0} \quad (3)$$

Where r is the radius in meters and r_f is the total radius. L_0 is sample length in meters and was measured directly after foaming. R_0 is the initial rotation in radians and was calculated from the number of initial rotations imposed on the fiber bundle. The average pitch, p, can also be quantified as the maximum possible circumferential shear strain.

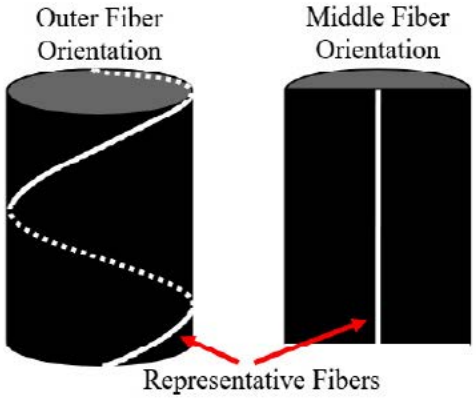

Figure 2: Radial orientation of outer fiber (Left), and middle fiber (right).

Cellular Stereological Analysis:

Samples for scanning electron microscopy (SEM) were prepared by cryofracture. Samples were notched and held in liquid nitrogen for 60 seconds then using a razor and hammer, were fractured axial and longitudinal to the CO_2 evacuation direction, described in **Figure 3**. Stereological analysis of the foam microporous structure was performed using Image-J analysis software on SEM micrographs taken on a Magellan 400 SEM. Each micrograph was converted to a black and white image and then the coloring was inverted. The particle analysis function was used to track the area, perimeter and best fit ellipse recording the ellipse area, major and minor axis. The diameter of each pore was calculated from the area of each pore assuming a perfect circle. An ellipse aspect ratio, RE, was calculated using Equation 4:

$$R_E = \frac{a}{b} \quad (4)$$

Where a and b are the ellipse major and minor axis respectively. A R_E value of 1 is considered a perfect circle and the further from one the more elliptical and anisotropic.

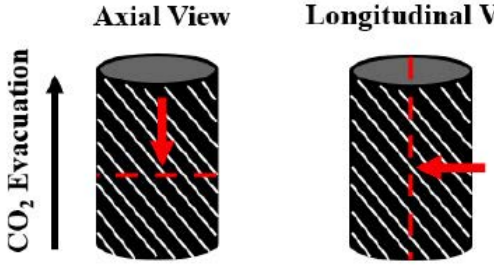

Figure 3: Naming of viewing angle relative to CO_2 evacuation direction.

The overall anisotropy value, R, of the microporous structure was determined using Figure 4 and Equation 5 [1]:

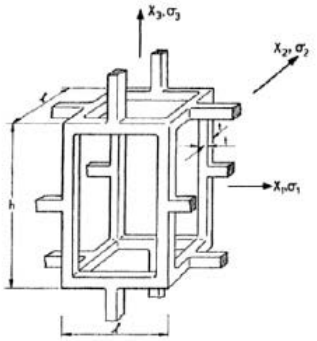

Figure 4: Idealized anisotropic pore strut model [1].

$$R = \frac{h}{l} \quad (5)$$

Where R is the overall anisotropy, h is the average height of the pores taken from the a-value of the longitudinal cross section, and l is the average cell diameter taken from the average of the a and b-values of the axial cross section, assuming perfect ellipsoidal pores.

Uniaxial Compression and Shear Strain Assembly:

Compression testing was performed using an Instron 5500R Mechanical Tester. PA 6 fiber bundle foams, with a helical bias, were compressed uniaxially in a shear strain assembly as shown in **Figure 5**. During compression these biased fiber bundle foams exhibit rotation along with axial deformation. The shear strain assembly allows for analysis of this rotation using a thrust ball bearing along with adhesive to only allow for rotation of the ball bearing, which can then be quantified as a circumferential shear strain, Y_{0z} in radians, which is calculated using Equation 7:

$$\gamma_{\theta z} = \frac{R * \Delta\theta}{H} \quad (7)$$

Where R is the sample radius, $\Delta\theta$ is the rotation during deformation in radians and H is the sample height in meters after rotation.

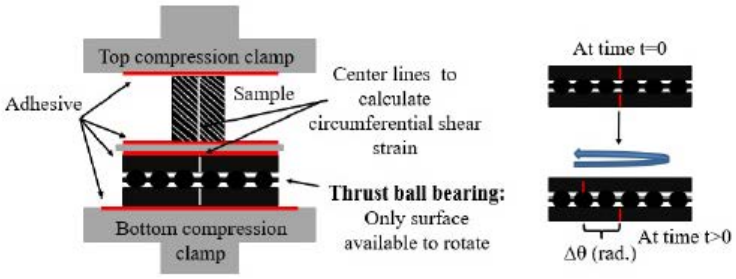

Figure 5: Shear strain assembly to track rotational deformation during compression for shear strain calculations.

Results & Discussion

The fiber used in this study is manufactured from PA6 as determined by DSC and FTIR (see Experimental Section). Polyamides have been shown to undergo a melt and crystallization depression when processed in shH2O, shown in **Figure 6**, with PA6 showing a melt depression of over 50°C,[21]. With the addition of water during the foaming process with $scCO_2$, the processing temperature can be drastically lowered, requiring less severe foaming and processing conditions. The fiber has a crystallinity of 21% and does exhibit a melt and crystallization depression.

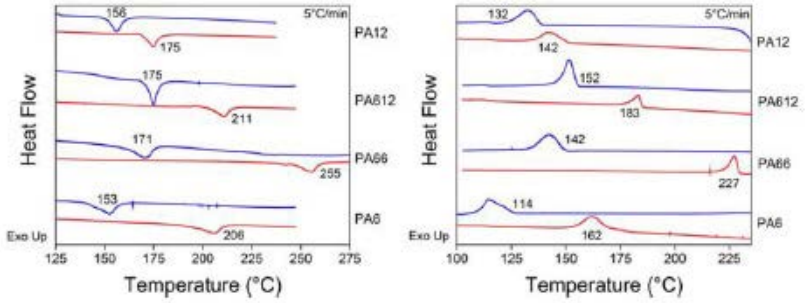

Figure 6: PA melting endotherms (Left) and crystallization exotherms (Right) with shH_2O (Blue) and without shH_2O (Red) with peak temperatures noted [21].

WAXS was conducted to quantify the degree of crystal orientation through Herma n's orientation factor, f, shown in Equation 1 and 2. **Figure 7** illustrates the 2D spectra that was used to calculate f along with a schematic of the different crystal orientations based on the calculated f value. A value of 0 results in a fully isotropic random orientation and ranges from -0.5 when all chains are perpendicular to the fiber directions and 1 when all the chains are aligned with the reference direction. The PA6 fiber has an f value of 0.11. While this shows low levels of molecular orientation, the fiber only contains 21% crystallinity, therefore a f value of 0.11 at this crystallinity shows the majority of crystals are aligned in the draw direction of the fiber.

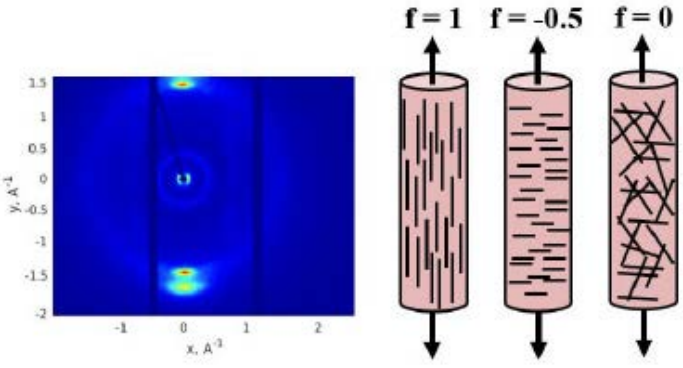

Figure 7: Trilene monofilament 2D WAXS pattern (Left) and Herma n's orienta tion function values with corresponding crystal alignment schematics (Right).

Cellular Stereological Analysis:

Oriented PA6 fibers foamed below the melt temperature have a microcellular structure with closed anisotropic cells that follow the fiber direction, regardless of fiber alignment to the evacuation of the CO2 and H2O. Figure 8 shows the microcellular structure of a sample foamed at the lower pressure and temperature conditions. The cells axial to the fiber are more isotropic with an average RE value of 1.2 with most of the cells having a value below 1.5. **Figure 8** also displays the microcellular structure longitudinal to the fiber, or following the fiber direction, with an overall RE value of 2.1, demonstrating a structural anisotropic cellular structure. Using Equation 5 the overall anisotropy R, can be calculated for the system and was found to be 2.1 demonstrating a highly structural anisotropic foam.

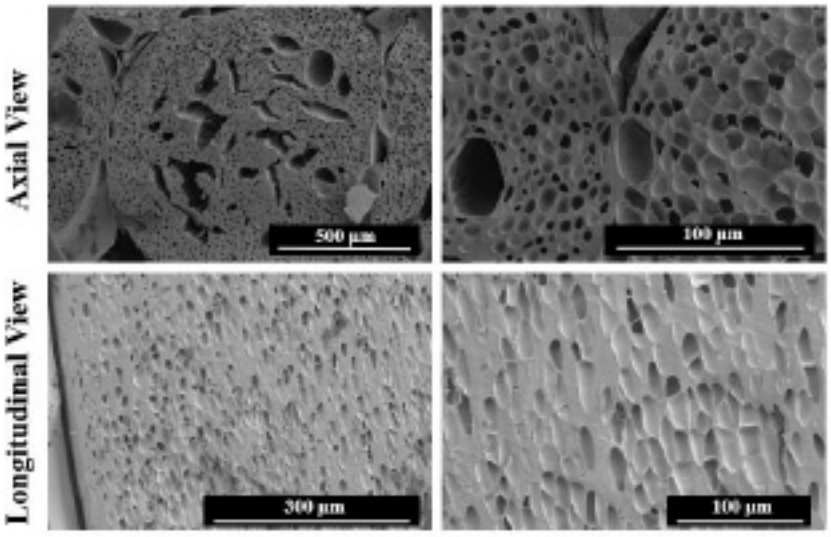

Figure 8: SEM micrographs of PA 6 fibers foamed in helical twist bias of 2 full rotations, at a pressure of 20.7 MPa and temperature of 108 °C.

Center radial fibers are not rotated around the sample but linearly twisted, while outer radial fibers undergo the full number of rotations imposed on the system described in Figure 2. The outer radial fibers consist of smaller less anisotropic cells with the average diameter and RE values being 13.7 µm and 1.8 respectively. The inner radial fibers have larger more anisotropic cells with an average diameter and RE value of 16.3 µm and 2.3 respectively. A possible explanation is that the anisotropy dictated by the molecular orientation works in concert with the traditional formation of anisotropic cells, producing higher levels of anisotropy. Traditionally anisotropy within microcellular structures is oriented in the direction of the release of confinement or direction of gas evacuation, which for center radial fibers aligns with the fiber direction.

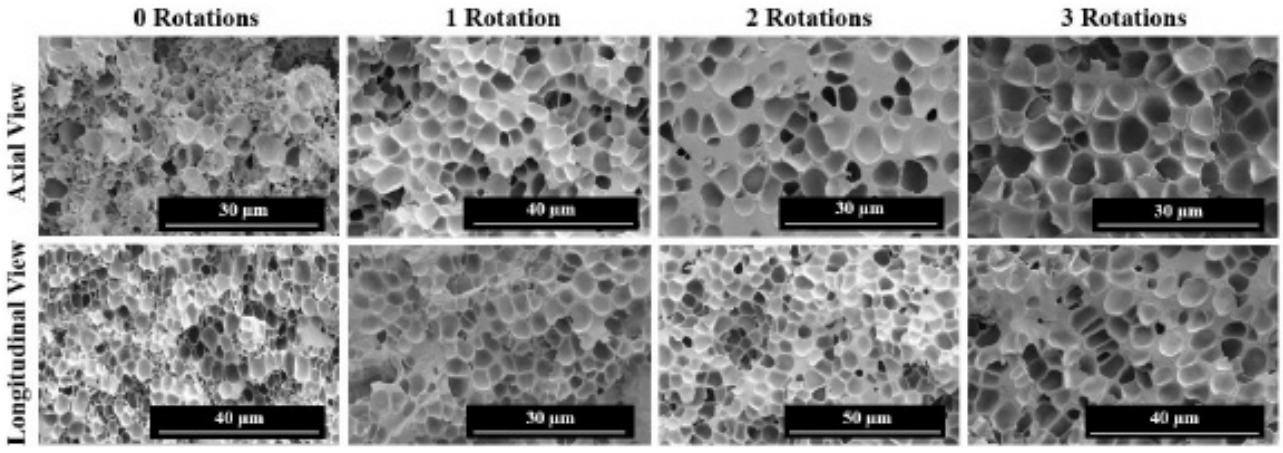

Figure 9: SEM micrographs of PA 6 fibers foamed with differing initial rotations at elevated foaming condition

The microcellular structure of PA6 fiber samples foamed at the higher pressure of 41.4 MPa are shown in **Figure 9**, with differing amounts of initial rotations imposed on each sample. An increase in temperature and/or pressure decreases the pore size and structural anisotropy [24]. An increase of CO_2 incorporation into the system results in the system being more highly supersaturated upon pressure evacuation. As the change in pressure during evacuation increases, the energy barrier to nucleation decreases resulting in a larger number of cells being nucleated within a given volume as predicted by homogeneous nucleation theory [24, 25].

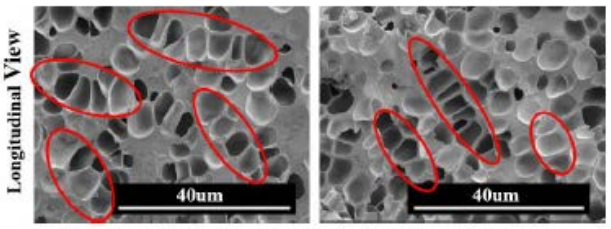

Figure 10: SEM micrographs of PA 6 fibers foamed at increased pressure of 41.4 MPa with cellular strings present and highlighted.

The average cell size is not heavily influenced by the change in rotations imposed on the system. The cells viewed axial to the fiber direction have average pore diameters ranging from 4.5-5.9 μm and average RE values of 1.3-1.4. longitudinal to the fiber orientation the average diameter and RE range from 3.4-55.2 μm and 1.3-1.4 respectively. The decrease in cell anisotropy is due to the increase in the number of cells nucleated. The increase in cell number density decreases the cell size by restricting cell growth, therefore hindering the formation of elongated anisotropic cells present in Figure 8.

Dissimilar to the lower pressure and temperature foamed samples that exhibit structural anisotropy, samples foamed at higher conditions exhibit material anisotropy in the form of cellular strings, shown in **Figure 10**. These samples have a smaller more isotropic microcellular structure; however, the cells align with thin walls in between them forming cellular strings. These cellular strings follow along the fiber direction, producing material anisotropy. Material anisotropy that aligns in the same direction as structural anisotropy will result in equivalent mechanical characteristics.

Uniaxial Compression and Complex Deformation:

PA6 fibers are bundled and fixed into a helical twist bias during foaming, creating an anisotropic template for the foam to generate within. The orientation of the crystal structure within the fiber helps dictate microcellular anisotropy, where the cells elongate along the fiber direction, producing a helically patterned anisotropic foam structure.

Sample	Initial Rotations	Avg. Pitch (rad.)	Density (g/cm^3)	Porosity	$\gamma_{\theta z}$ (rad.)
1	2	0.30	0.226	77%	0.25
2	2	0.30	0.581	51%	0.08

Table 2: Density and circumferential shear strain of PA 6 fibers foamed in helical twist bias of 2 full rotations, at a pressure of 20.7 MPa and temperature of 108 °C.

These helically patterned foams undergo rotation during uniaxial compression demonstrating a complex deformational response. This rotation is quantified as circumferential shear strain, $\gamma\,\theta Z$, and is calculated using Equation 7. The average pitch, calculated from Equation 3 with values shown in Tables II and III, is a representation of the average rotations each fiber undergoes throughout the radius, with respect to the fiber length. This can also be better understood as the maximum possible circumferential shear strain each sample could undergo during compression.

Within **Table 2** are examples of PA6 fiber foams, foamed at lower conditions with 2 initial rotations imposed on the system. These samples had more variability in the foam density and $\gamma\,\theta Z$ due to low reproducibility caused by the small processing window and low $scCO_2$ solubility into the system. Table III shows samples foamed at higher pressures and with differing amounts of initial rotations. As the number of initial rotations increases from 0, 1, 2 or 3, the $\gamma\,\theta Z$ increases to 0.00, 0.13, 0.19 and 0.25 radians respectively.

As the number of initial rotations increases, the deviation between γ,θZ and p increases. This was not investigated but could be due to many things. The increase in rotations adds stress on the fibers and therefore have to be foamed at lower temperatures as shown in Table III. The change in temperature or applied stress, during foaming, can impa ct the fina l foam's ability to rotate. Also, the change in temperature can impact the amount of welding between the fibers. A change in the fiber welding does not hinder the rotation but can lead to premature failure if the fibers are not fully welded.

Initial Rotations	Avg. Pitch (rad.)	Foaming Temp. (°C)	Density (g/cm^3)	Porosity	$\gamma_{\theta z}$ (rad.)
0	0	128	0.650	45.5%	0.00
1	0.15	125	0.608	49.0%	0.13
2	0.30	123	0.603	49.4%	0.19
3	0.45	123	0.682	42.7%	0.25

Table 3: Density and circumferential shear strain of PA 6 fibers foamed with differing initial rotations, at a pressure of 41.4 MPa and variable temperatures.

Conclusions

Oriented PA6 commodity fibers can be foamed in $scCO_2$ and shH_2O at temperatures below the melting point, only foaming within the amorphous regions. This results in a closed pore foam where pore number density and size can be altered with changes in foaming conditions. PA6 fiber foaming occurs at relatively low temperatures due to melt depression caused by shH2O. The solubility parameter of scCO2 increases with increasing pressure, increasing its miscibility with PA6, and broadening the temperature processing window for more reproduceable foaming.

The molecular orientation of the fiber dictates the direction of the microcellular structure anisotropy. Fiber bundles with an imposed helical twist during foaming exhibit elongated cells that follow along the fiber direction at lower processing pressures, producing a high level of structural anisotropy with R = 2.1. Cell size and anisotropy is not homogeneous throughout the fibers. Outer radial fibers undergo the full number of applied rotations and exhibit smaller less anisotropic cells, while center radial fibers cells are larger and more anisotropic. This increase in size and RE for middle fiber cells is due to the combination of anisotropy forming in the direction of confinement release working in concert with anisotropy formed along the fiber orientation.

At higher processing pressures, the cell size and anisotropy decrease. The cells, however, do attempt growth and elongation, forming thin walls between them along the fiber orientation direction. This results in material anisotropy in the form of cellular strings.

Oriented PA6 fiber bundles with an imposed bias of a helical twist, have anisotropy that follows the helical pattern of the fibers. The helically patterned anisotropy results in a rotational response during uniaxial compression, which is a form of complex deformation. The rotational response is quantified as the circumferential shear strain, which increases as the initial rotations imposed on the system increase.

An imposed bias on a semicrystalline polymer template during foaming develops a microcellular structure with anisotropy following the template bias. This complex anisotropic microcellular structure results in a complex deformational response. This study investigates only PA6 fibers templated into a helical twist, however there is an abundance of oriented polymers that can be foamed in many different biases to engineer in a wide array of complex deformational behaviors.

Acknowledgments

We thank Matthias Hartmann and all of PUMA (Herzogenaurach Germany) for providing financial support and thoughtful discussion for this work.

References

1. L. J. Gibson and M. F. Ashby, Cellular Solids, Cambridge University Press (1997).
2. Cork, Elsevier (2007).
3. F. L. Jin, M. Zhao, M. Park, and S. J. Park, Polymers (Basel). 11 (2019).
4. S. Deville, Scripta Materialia 147, 119 (2018).
5. S. Wang, G. Wang, X. Zhang, Y. Tang, J. Wu, X. Xiang, X. Zu, and Q. Yu, Carbon 120, 103 (2017).
6. V. Bernardo, E. Laguna -Gutierrez, A. Lopez-Gil, and M. A. Rodriguez-Perez, Mater. Des. 114, 83 (2017).
7. G. Coste, C. Negrell, and S. Caillol, Eur. Polym. J. 140, 110029 (2020).
8. A. T. Huber and L. J. Gibson, J. Mater. Sci. 23, 3031 (1988).
9. L. Sorrentino, E. Di Maio, and S. Iannace, J. Appl. Polym. Sci. 116, 27 (2010).
10. V. Shaayegan, C. Wang, M. Ataei, F. Costa, S. Han, M. Bussmann, and C. B. Park, J. CO2 Util. 51, 101615 (2021).
11. E. Reverchon and S. Cardea, J. Supercrit. Fluids 40, 144 (2007).
12. H. Sun and J. E. Mark, J. Appl. Polym. Sci. 86, 1692 (2002).
13. L. Sorrentino, M. Aurilia, and S. Iannace, Adv. Polym. Technol. 30, 234 (2011).
14. T. Xia, Z. Xi, T. Liu, and L. Zhao, Chem. Eng. Sci. 168, 124 (2017).
15. J. Reignier, R. Gendron, and M. F. Champagne, J. Cell. Plast. 43, 459 (2007).
16. A. Salerno, E. Di Maio, S. Iannace, and P. A. Netti, J. Supercrit. Fluids 58, 158 (2011).
17. L. M. Matuana, Bioresour. Technol. 99, 3643 (2008).
18. K. A. Neavor, A. J. Lesser, and T. J. McCarthy, Am. Chem. Soc. Polym. Prepr. Div. Polym. Chem. 38, 446 (1997).
19. S. Owusu-Nkwantabisah, C. Staudt, and A. J. Lesser, Polym. Eng. Sci. 58, 1108 (2018).
20. G. Guenoun, N. Schmitt, S. Roux, and G. Régnier, Polym. Eng. Sci. 61, 107 (2021).
21. G. C. Evans and A. J. Lesser, J. Polym. Sci. Part B Polym. Phys. 56, 803 (2018).
22. L. L. Williams, J. B. Rubin, and H. W. Edwards, Ind. Eng. Chem. Res. 43, 4967 (2004).
23. L. L. Williams, Hansen Solubility Parameters A Users Handbook, Second Ed., CRC Press, 177 (2007).
24. S. K. Goel and E. J. Beckman, Polym. Eng. Sci. 34, 1137 (1994).
25. S. K. Goel and E. J. Beckman, Polym. Eng. Sci. 34, 1148 (1994).

IMD Board of Directors Meeting
March 22nd, 2024 – Virtual

Meeting minutes taken and submitted by Davide Masato (2023-2024 SPE IMD Secretary).

Welcome & Opening Remarks (David Okonski / Jeremy Dworshak)

Roll Call: 20 16 active board members on roster: quorum achieved.

Meeting begins with intro about the agenda, and a quick update on the last meeting, strategy. Thoughts on ANTEC: Are we happy? What would we like to change? What not to change? What`s the IMD role? Reception? What`s the outcome?

Approval of previous Meeting Minutes (Davide Masato)
Motion: Approval of previous meeting (20231214, Virtual). Motion (Davide Masato). Seconded by Edwin Tam. No discussion. All in favor.

Reports Discussion

Councilor meeting (Edwin Tam)

- Workshop for groups divided into tables. Questions about concerns for SPE. They plan to report in April. Concerns about only one meeting last year, difficult to give feedback to HQ.
- No one leads the council. Can change in the future. As of now is difficult to give feedback if not individually.

ANTEC (Tom Giovanetti):

- Tom was moderator for 12 papers. Attendance: 34, 31, 27, 25, 17, 28, 19, 22, 11, 14, 18, 16. Some papers were not excellent. The discussion was good from the audience.
- Advice for the next TPC: transition with reviewing the papers together.

Action: Which papers can be invited for AutoEPCON? Can we connect with other divisions about how to organize the session?

Workshops (Kusuma/Ulven)

Meetings to discuss workshops with interested BODs and discussins on how to get things started.

Internally and externally focused discussions. The idea is to serve all plastics professionals even if they are not members. Provide support to students. Make potential income for the IMD division. The next event will be standalone before we, in the future, partner with other groups. We want to make sure that the IMD gets credit for the event.

- **Week of Molding**: • New technologies • Sustainability
- **Connect with the Extrusion Division:** • Learn from them • Partner with them on some programs.

- Partner with Moldex3D?
- Learn from Penn State event? Joint event? Conference already has workshops.
- Automotive Division AutoEPCON? Launching point?
- We can use information from the Membership to focus on standalone events. What is the format?

Action: Let David Kusuma know if you`d like to join the committee.

Sustainability (Masato/Kleczek)

Invite speakers (suggestion: Conor Carlin). Monika will be on maternity leave but will continue to help identifying speakers and has connected Jeremy with a colleague (Marica Pires).

Communications (Rodenburgh/Foltz)

Plan in progress for the LinkedIn page which will go live in May/June.

- BOD in academia – please consider speaking roles or, suggest topics.
- Which speakers should be invited? Old presentations ranged from simple to more advanced. We want to make sure that attendees know what to expect from the event.

Action: Need to prepare the agenda for the two-day week of injection molding.

New Business

Motion: (Edwin Tam) for week of molding on 9/24-25. Seconded by Tom G. Motion carries with all in favor.

Motion: (Edwin Tam) on updating the mission of the IMD. Seconded by Joseph Lawrence. Motion carries with all in favor.

Motion: (Srikanth) on updating the objective of the IMD. Seconded by Tom G. Motion carries with all in favor

- *Should TPC be an officer?* First reading. The role is pivotal and then moves into an officer position. We will be voting at our next meeting. Can we add an observer to the officers? We will think about this.
- *Linkedin page:* Motion on creating a public company Linkedin page and maintain the private group (Edwin Tam). Seconded by Edwin Tam. Motion carries with all in favor. Volunteers needed to be admins of the page? Angela, Jeremy.
- *Board elections:* Motion to approve officers (Edwin Tam). Seconded by Joseph Lawrence. Motion carries with all in favor. Nominations for the general ballot. Officers don`t have to be elected. Motion to approve BOD nominees (Edwin Tam). Seconded by Joseph Lawrence. Motion carries with all in favor. Send a short bio for the nomination ballot to Hoa Pham. We need volunteers for 2026 and forward and need to remember that we roll off the board after 9 years of service. Speak with David Kusuma about inviting new board members.
- *AM Conference – Susan:* Conference scheduled in Cleveland, 10/17/2024. Weneed suggestions for speakers and support with sharing the event information. Susan will send the information to the board.
- *ANTEC 2025 in Philadelpia:* BOD at ANTEC at the University of Delaware hosted by Srikanth Pilla. David Kusuma will consider the offer. Should we have a shared folder? (Create a mailing list?, Google drive? Or others?)

Next meeting will be virtual in June: Officers meeting and committee meetings will happen until then. **Meeting Adjourned at 2.32 pm EST**

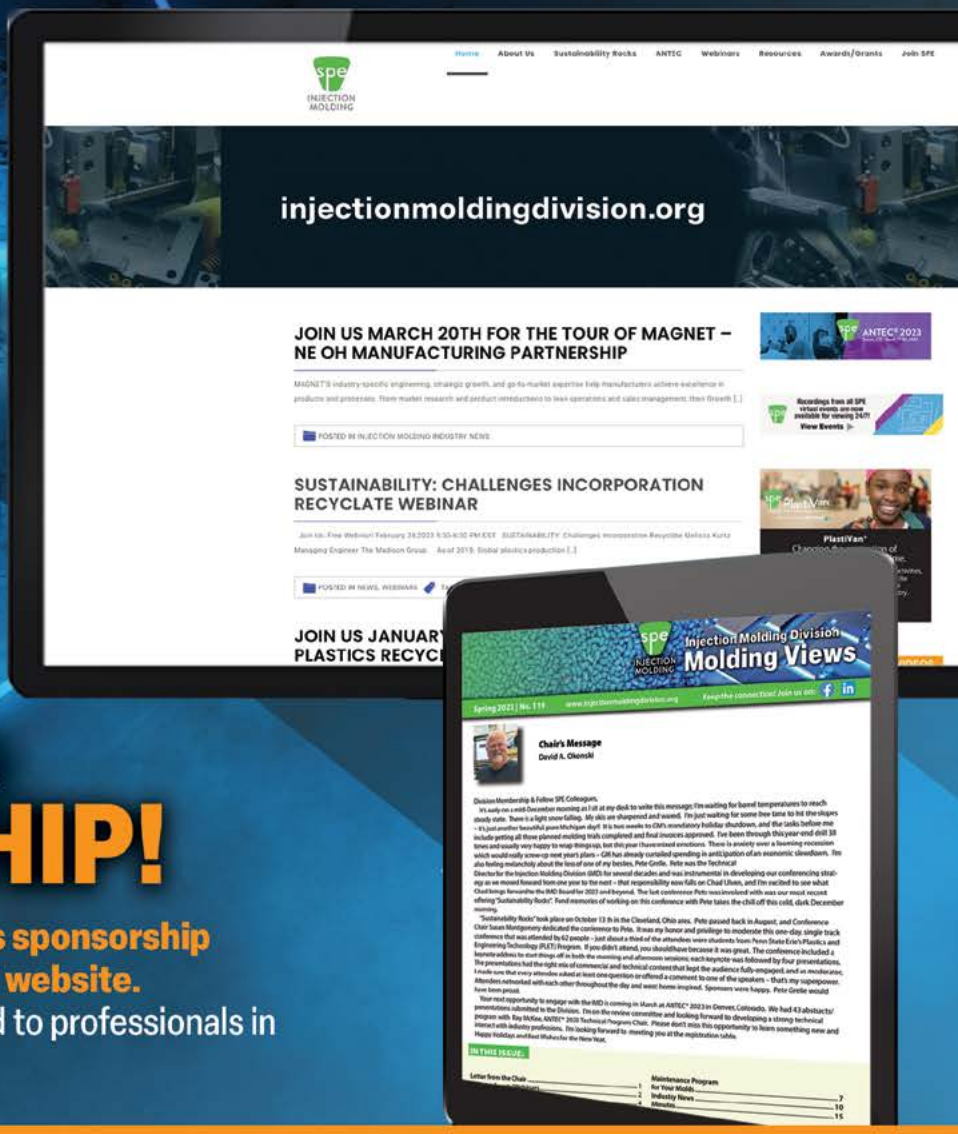

spe
INJECTION MOLDING

REACH YOUR TARGET AUDIENCE AND GROW YOUR BUSINESS WITH A SPONSORSHIP!

The Injection Molding Division offers sponsorship advertising with the newsletter and website.
Reach the IMD membership with your ad to professionals in the injection molding industry.

The SPE Injection Molding Division Newsletter readership is composed of individuals involved in all aspects of the injection molding industry. These issues are made possible through the support of sponsors shown in this Newsletter and injection molding website.

OPTION 1: $2,500/yr
- Full page ad placed in 3 newsletters
- Side Button on website for the year
- First right of refusal for tabletop at ANTEC
- Company logo recognizion on signage at SPE IMD events
- Plastchick interview
- Technical article in newsletter & website
- Company press releases for website, social media and newsletter

OPTION 2: $1,500/yr
- Half page ad placed in 3 newsletters
- Side Button on website for the year
- Company logo recognizion on signage at SPE IMD events
- Technical article in newsletter & website
- Company press releases for website, social media and newsletter

OPTION 3: $1,000/yr
- Full page ad placed in 3 newsletters
- Side Button on website for the year
- Company press releases for website, social media and newsletter

OPTION 4: $750/yr
- Half page ad placed in 3 newsletters
- Side Button on website for 6 months
- Company press releases for website, social media and newsletter

OPTION 5: $450/yr
- Half page ad placed in 1 newsletter
- Side Button on website for 3 months

To schedule your ad contact: publisherIMDNewsletter@gmail.com

Division Officers:

Chair:	Jeremy Dworshak (3M)
Chair-Elect:	David Kusuma
Treasurer:	Raymond McKee (Currier Plastics)
Secretary:	Davide Masato
Technical Director:	Chad Ulven
Education Committee Chair:	Srikanth Pilla (Clemson University)
Past Chair:	David Okonski
Councilor:	Edwin Tam
ANTEC TPC:	Tom Giovannetti
Membership	Erik Foltz
Nominations:	Hoa Pham
Communications:	Angela Rodenburgh
Scholarship:	Lynzie Nebel
Education:	Srikanth Pilla
Sponsorships:	Sriraj Patel
TopCon Chair - Penn State Plastics Conference:	Brad Johnson
HSM & Fellows:	Lih-Sheng (Tom) Turng
Board Member:	Saeed Farahani
Board Member:	Joseph Lawrence
Board Member:	Vikram Barghava
Board Member:	Alex Beaumont
Board Member:	Kishor Mehta
Board Member:	Larry Geist
Board Member:	Davide Masato

HASCO Portal – USA and Canada

As a leading global manufacturer of standardized, modular quality mold units and individually specialized hot runner systems, HASCO offers innovative and economical solutions for designers, mold makers and injection molders from a single source.

At www.hasco.com, customers have access to the online shop and the company website. Starting May 2024, our customers in the US and Canada will be able to benefit from all the advantages of the HASCO Portal. With just a few clicks, they can find exactly what they need among 100,000 standard mold components, plates, mold bases and hot runner systems.

It is fast, simple, clear, and complete, so that all information, innovations, and services can be called up in one system. Molds can be calculated, configured, and ordered directly around the clock with just a few clicks. The HASCO mold base assistant offers innovative possibilities to simplify and accelerate processes.

Intelligent product search

A performance-oriented product navigation with extensive full-text search enables the desired article to be reliably found. Inquiries relating to product availability can be answered instantly.

Fast mold configuration

With the mold structure assistant, individual shapes can be configured in just 5 steps. The design process is clearly presented and allows access to the complete range of ready-to-install system components.

Simple cost calculation

Parts lists are generated via the simple, individual cost calculation – even for custom-made products – and the complete order is sent directly to HASCO for processing with one click.

Direct interface to common CAD systems

Designers benefit from the fast download of CAD data via interfaces to more than 40 different data formats. CAD direct insertion drivers ensure the convenient import of 3D data into various CAD systems. The practical BOM export for calculation and ordering is particularly simple and fast in daily use.

Live access to quotes and orders

In the respective customer account, all customer-specific information is available and inquiries and orders are transparently displayed in an overview with the respective processing status.

At www.hasco.com, mold makers can use one of the most modern and powerful customer portals in the industry. All products, innovations and services are available worldwide in the HASCO Portal 24/7.

spe®

INJECTION MOLDING

Top Reasons to Join SPE and its Injection Molding Division

JOIN!

Benefits include:

Discounts to SPE Live Webinars and Events!
Technical Journals – FREE
Digital Access to Plastics Engineering Magazine
SPE News
Online Directory Access
Listing in Member Director
Salary Survey
Weekly Plastics Insight Newsletter
Access to SPE Communities - formerly The Chain
Eligible for Committee & Chapter Participation, including Voting
Access to the Materials DatabaseLIG Association Health Program
And More!

Visit www.4spe.org to join today.

Progressive Components Introduces New M-2 Ejector Pins

Progressive Components announces the release of its new M-2 Ejector Pins, which are especially suited for high wear resistance with abrasive materials.

Engineered and manufactured to meet the demanding conditions of today's injection molds, Progressive's Ejector Pins feature tight tolerances held for sizing, roundness, and straightness.

Expanding its extensive line of ejector pin options, the new M-2 Ejector Pin is manufactured from M-2 tungsten-molybdenum high-speed steel and hardened to 60-63HRC, which at its through-hardened core provides wear resistance against dishing when molding abrasive materials.

Ideal for accepting contours with high surface-finish requirements, M-2 Pins can be used as either ejector pins or core pins and are suited for high-heat applications.

Progressive's M-2 Pins are available in straight and shoulder versions. Straight pin diameters range between 1/32" and 1/2", with lengths between 3" and 18". Shoulder Pin diameters range between 1/32" and 7/64", with 1/2", 2", or 3" shoulders and 6" or 10" lengths. Keyed, cut-to-length, and custom options are also available.

For more information on M-2 Ejector Pins or any other exclusive mold components, visit www.procomps.com, email tech@procomps.com, or call 1-800-269-6653.

Progressive Components | 1-800-269-6653 | procomps.com